Math. Model. Nat. Phenom. 20 (2025) 1
https://doi.org/10.1051/mmnp/2024023

**Mathematical Modelling of Natural Phenomena**
www.mmnp-journal.org

# WAVE PROPAGATION ALONG THE INTERFACE BETWEEN THE HYPERBOLIC GRADED-INDEX AND PHOTOREFRACTIVE CRYSTALS

S.E. Savotchenko[1,2,3,*]

**Abstract.** New two types of transverse interface waves propagating along the planar contact the photorefractive and hyperbolic graded-index crystals are described theoretically. The waves are given by exact analytical solutions to the stationary wave equations with spatial dependent coefficients. The waves of the two types differ from each other by the presence of oscillations of the decaying field profile in the photorefractive crystal and the range of existence. Influence on the wave profiles of the system parameters such as the effective refractive index, temperature, and the hyperbolic profile parameters (the interface refractive index, and the characteristic distance) are analyzed in details. New features of the distribution of the maxima and minima of the field profile and the depth of its penetration into crystals depending on the values of these parameters are specified.

**Mathematics Subject Classification.** 00A79.

Received September 27, 2024. Accepted November 9, 2024.

## 1. Introduction

Localized structures in optical media are studied actively recent years [1–3]. Various types of surface waves in photorefractive crystals with different types of nonlinear response formation are described theoretically for a long time by many authors [4–7].

Of particular interest are surface waves propagating along the boundaries of photorefractive crystals and crystals with other optical properties [8–14]. A model of the formation of a nonlinear response by means of a diffusion mechanism is often used in the theoretical description of waves in photorefractive crystals [15–18].

Waves along the contact of such a crystal with media, in which the refractive index depends on the distance from the contact surface, have been studied comparatively little and therefore require additional and more detailed investigations. Such media, in which the refractive index depends on the spatial coordinate, are called gradient or graded-index media [19–22].

An important role in such studies is played by the problem of obtaining exact analytical solutions to the wave equation with spatially distributed coefficients [23–25]. Special methods are used that allow solutions to

*Keywords and phrases:* Nonlinear optics, nonlinear surface waves, photorefractive crystal, hyperbolic graded-index medium, inhomogeneous refractive index, hyperbolic index profile.

[1] MIREA – Russian Technological University, Vernadsky Ave., 78, 119454 Moscow, Russia.
[2] Russian Sergo Ordzhonikidze State Geological Prospecting University Miklukho-Maklaya St., 23, 117997 Moscow, Russia.
[3] Moscow Technical University of Communications and Informatics, Aviamotornaya St., 8a, 111024 Moscow, Russia.

[*] Corresponding author: savotchenkose@mail.ru

be obtained for the case of an arbitrary spatial distribution of the refractive index to describe waves in such media [26–31] including bilayer waveguides [32]. In particular, optical solitons are described using nonlinear forms using Kudryashov's approach [33, 34], including parabolic–nonlocal combo nonlinearity [35]. Also the highly dispersive optical solitons are reported [36–38]. Models in optical fibers with power-law of self-phase modulation are presented in [39–41]. Solutions of resonant nonlinear Schrödinger equation with exotic non-Kerr law nonlinearities are obtained in [42].

It should be noted that at present there are many technologies for obtaining refractive index profiles that decrease with distance from the surface in different media [43, 44] including phonic crystal structures [45–48].

In our study we will be interested in the so-called hyperbolic profile [49, 50] where the hyperbolic graded-index materials embedded in one-dimensional photonic crystals were considered in the framework of the photonic band-gaps engineering. A hyperbolic graded-index biophotonic cholesterol sensor with improved sensitivity was presented in [51]. Thus, surface waves in optical media with a hyperbolic profile of the refractive index require more detail investigations [52].

In this paper, we theoretically study the interface waves propagating along the contact the hyperbolic graded-index and photorefractive crystals. Surface waves along the contact of a photorefractive crystal with a diffusion mechanism of nonlinearity formation with media characterized by other refractive index profiles were considered by us earlier [53–55] including layered structures [56–58]. Recently we present new exact solutions to the wave equations describing the surface waves propagating along the hyperbolic graded-index medium contacting with Kerr nonlinear medium [59] and medium with a step change in the dielectric constant [61]. Therefore, the present paper can be considered as a continuation of investigation of surface waves in hyperbolic graded-index media where new solutions are presented and new peculiarities of transverse wave profiles are described in the case on the contact with the photorefractive crystal.

## 2. Governing equations

Let us consider the flat interface at $x = 0$ plane between the photorefractive crystal with diffusion type of nonlinearity ($x < 0$) and the crystal with a hyperbolic spatial profile of the refractive index (hyperbolic graded-index crystal, $x > 0$). We describe the stationary transverse magnetic wave propagating along $z$ axis with the component of magnetic field

$$H_y(x,z) = \mathrm{e}^{i\beta z} H(x), \tag{2.1}$$

where $\beta = k_0 n$ is the propagation constant, $k_0 = 2\pi/\lambda_0$ is the wave number, $\lambda_0$ is the wavelength, $n$ is the unknown effective refractive index, $H(x)$ is the transverse distribution of the magnetic field. It can be found the stationary wave (Helmholtz) equation [21, 22]:

$$H''(x) = k_0^2\{n^2 - n_{cr}^2(x,I)\}H(x), \tag{2.2}$$

where $I \sim |H|^2$ is the magnetic field intensity, the $n_{cr}(x,I)$ is the inhomogeneous nonlinear refractive index of the contacting crystals, which is given by

$$n_{cr}(x,I) = \begin{cases} n_{ph}(I), \ x < 0, \\ n_{hy}(x), \ x > 0, \end{cases} \tag{2.3}$$

where $n_p(I)$ and $n_h(x)$ are the refractive indices of the photorefractive crystal and the hyperbolic graded-index crystal respectively.

In this paper, we propose the following index profile (we call it a hyperbolic profile because the dielectric function is $\varepsilon = n_{cr}^2(x, I) \propto 1/x$):

$$n_{hy}(x) = \frac{n_0}{\sqrt{1 + x/h}}, \tag{2.4}$$

where $n_0 = n(0)$ is the refractive index at the crystal interface (the interface refractive index), $h$ is the characteristic distance from crystal interface, at which the value of the refractive index at the interface decreases by $2^{1/2}$ $n(h) = n_0/\sqrt{2}$ (we call $n_0$ and $h$ the hyperbolic index profile parameters).

We use the following refractive index in the photorefractive crystal:

$$n_{ph}(I) = n_{p0} + \Delta n_{ph}(I), \tag{2.5}$$

where $n_{p0}$ is the unperturbed (constant) refractive index of the photorefractive crystal, and $\Delta n_{ph}(I)$ is its intensity dependent perturbation, which is assumed to be a small one: $\Delta n_{ph}(I) \ll n_{p0}$.

The index perturbation in the case of a diffusion mechanism of nonlinearity formation in the photorefractive crystal is given by [15–17]

$$\Delta n_{ph}(I) = -\frac{1}{2} n_{p0}^3 r_{eff} \frac{k_B T}{e} \frac{I'}{I + I_d}, \tag{2.6}$$

where $r_{eff}$ is the effective electro-optic coefficient, $k_B$ is Boltzmann constant, $T$ is a temperature, $e$ is the electron charge modulus, $I_d$ is the dark intensity.

We find combining equations (2.2)–(2.6) that the transverse distribution of the magnetic field in the photorefractive crystal in the case of $I_d \ll I$ obeys the equation:

$$H''(x) - 2\mu H'(x) + k_0^2(n_{p0}^2 - n^2)H(x) = 0, x < 0, \tag{2.7}$$

where, $\mu = k_0 T/T_p$ is the photorefractive crystal damping factor, $T_p = e/k_0 k_B r_{eff} n_{p0}^4$ is the characteristic temperature [56, 57].

Note that the photorefractive crystal damping factor $\mu \sim T$. Therefore, we can obtain required interface wave characteristics by the temperature varying [61].

The transverse distribution of the magnetic field in the hyperbolic graded-index crystal obeys the equation:

$$H''(x) + k_0^2 \left( \frac{n_0^2}{1 + x/h} - n^2 \right) H(x) = 0, x > 0. \tag{2.8}$$

We add the following boundary conditions at the crystal interface plane $x = 0$:

$$H(+0) = H(-0) = H_0, H'(+0)/n_0^2 = H'(-0)/n_{p0}^2 \tag{2.9}$$

where $H_0$ is the interface amplitude, and $|H(x)| \to 0$ at $|x| \to \infty$.

Thus, we formulate the boundary problem (2.7)–(2.9), the solutions to which describes the interface waves propagating along the contact of the photorefractive crystal with diffusion type of nonlinearity and the crystal with a hyperbolic spatial profile of the refractive index.

## 3. Interface waves: exact solutions

We find limited and disappearing at $x \to +\infty$ exact solution to equation (2.8)

$$H(x) = H_0 \frac{W_{m,1/2}(2nk_0(x+h))}{W_{m,1/2}(2nk_0h)}, x > 0, \tag{3.1}$$

where $W_{m,1/2}(x)$ is the Whittaker function [62] and $m = hk_0n_0^2/2n$.

The solution to equation (2.7) at $x < 0$ can be written as

$$H(x) = H_0 \mathrm{e}^{\mu x} \begin{cases} \dfrac{\cosh(\nu x + \delta)}{\cosh(\delta)}, \ n_b < n < n_{p0} \\ \dfrac{\cos(px + \varphi)}{\cos(\varphi)}, \ n < n_b \end{cases}, \tag{3.2}$$

where

$$n_b = \sqrt{n_{p0}^2 - T^2/T_p^2} \tag{3.3}$$

is the value of the refractive index, at which the change in the types of the waves occurs;

$$\nu^2 = k_0^2\{(T/T_p)^2 - n_{p0}^2 + n^2\}, \tag{3.4}$$

$$p^2 = -\nu^2 = k_0^2\{n_{p0}^2 - n^2 - (T/T_p)^2\}, \tag{3.5}$$

and the values of $\delta$, and $\varphi$ are determined by the boundary conditions (2.9).

Note that the solutions (3.1), and (3.2) satisfy the first boundary condition (2.9) corresponding to the field continuity. To satisfy the second boundary condition (2.9), we substitute equations. (3.1), and (3.2) into equation (2.9) and obtain the following values of $\delta$, and $\varphi$:

$$\delta = \tanh^{-1}\left(\frac{\gamma - \mu}{\nu}\right), \tag{3.6}$$

$$\varphi = \tan^{-1}\left(\frac{\mu - \gamma}{p}\right), \tag{3.7}$$

where

$$\gamma = q_G n_{p0}^2/n_0^2,$$

$$q_G^2 = (n^2 - n_h^2)k_0^2,$$

$$n_h^2 = n_{he}(2n - n_{he}),$$

$$n_h = \frac{n_0^2}{2n} + \frac{W_{m+1,1/2}(2nk_0h)}{k_0hW_{m,1/2}(2nk_0h)}.$$

Thus, we find two types of interface waves as exact solutions of the boundary problem (2.7)–(2.9). The first one is given by

$$H(x) = H_0 \begin{cases} \dfrac{W_{m,1/2}(2nk_0(x+h))}{W_{m,1/2}(2nk_0h)}, x > 0 \\ \mathrm{e}^{\mu x}\dfrac{\cos(px+\varphi)}{\cos(\varphi)},\ n < n_b,\ x < 0 \end{cases} \tag{3.8}$$

and the second one is given by

$$H(x) = H_0 \begin{cases} \dfrac{W_{m,1/2}(2nk_0(x+h))}{W_{m,1/2}(2nk_0h)}, x > 0 \\ \mathrm{e}^{\mu x}\dfrac{\cosh(\nu x+\delta)}{\cosh(\delta)},\ n_b < n < n_{p0},\ x < 0 \end{cases} \tag{3.9}$$

The parameters of the waves (3.8) and (3.9) are determined by equations. (3.4)–(3.7). They can be controlled by two physical quantities such as the effective refractive index and the crystal temperature, which are easily changed in experiments. Note that the effective refractive index is determined by the angle of incidence of the beam exciting the interface wave.

The interface wave of the first type determined by equation (3.8) attenuates with oscillation in the photorefractive crystal with the spatial period $\Lambda = 2\pi/p$. Not that the value of $\Lambda$ can be also controlled by the effective refractive index and the crystal temperature in accordance with equation (3.5).

The interface wave of the second type determined by equation (3.9) attenuates without oscillation in the photorefractive crystal. Such waves can propagate in a photorefractive crystal with a diffusion type of nonlinearity at small angles of incidence of the beam exciting this wave.

Both types of the interface waves penetrate in the photorefractive crystal at the characteristic distance (penetration depth) $l_p = 1/\mu = T_p/Tk_0$. Therefore, we can reduce the penetration depth of the field into the photorefractive crystal by increasing the temperature.

We determine the total power flow carried by the guided waves as:

$$P = \int_{-\infty}^{+\infty} |H(x)|^2\,\mathrm{d}x = P_{ph} + P_{hy}, \tag{3.10}$$

where

$$P_{ph} = \int_{-\infty}^{0} |H(x)|^2\,\mathrm{d}x \tag{3.11}$$

is the part of the power flow in the photorefractive crystal, and

$$P_{hy} = \int_{0}^{\infty} |H(x)|^2\,\mathrm{d}x \tag{3.12}$$

is the part of the power flow in the hyperbolic graded-index crystal.

We substitute equation (3.1) into equation (3.12) and obtain

$$P_{hy} = \frac{H_0^2 J_m(2nk_0h)}{2nk_0 W_{m,1/2}^2(2nk_0h)}, \tag{3.13}$$

where

$$J_m(s) = \int_s^{\infty} W^2_{m,1/2}(t)\mathrm{d}t.$$

We substitute equation (3.2) into equation (3.12) and obtain

$$P_{ph} = \frac{H_0^2}{4}\begin{cases} \dfrac{1}{\cosh^2(\delta)}\left\{\dfrac{1}{\mu} + \dfrac{\mu\cosh(2\delta) - \nu\sinh(2\delta)}{\mu^2-\nu^2}\right\},\ n_b < n < n_{p0} \\ \dfrac{1}{\cos^2(\varphi)}\left\{\dfrac{1}{\mu} + \dfrac{\mu\cos(2\varphi) + p\sin(2\varphi)}{\mu^2+p^2}\right\},\ n < n_b \end{cases}, \tag{3.14}$$

We calculate and analyze the confinement factors in the photorefractive and hyperbolic graded-index crystals using equations (3.13), and (3.14) respectively [63]:

$$\Gamma_j = P_j/P, j = hy, ph. \tag{3.15}$$

The confinement factors of the transverse modes show that the transverse electromagnetic field must be localized in any propagation mode in the corresponding region of the crystal along the waveguide interface and shows how efficiently transverse electromagnetic waves propagate through the interface without losses. In the analysis under consideration, the confinement factors help to identify the areas of the crystal along the waveguide, in which the magnitude of the power flow of the interface wave will be the greatest one.

## 4. Results analysis

Characteristic profiles of the interface waves of the first type given by equation (3.8) are presented in Figure 1. We find that the wave intensity and maximum/minimum positions are determined by the sign of the phase $\varphi$ given by equation (3.7). The one maximum is observed in the hyperbolic graded-index crystal when the phase is a negative one and the one minimum is observed when the phase is a positive one. We analyze numerically effect of the system parameters such as the effective refractive index $n$, temperature $T$, hyperbolic profile parameters: the interface refractive index $n_0$ and the characteristic distance $h$.

Figure 1a demonstrates the influence of the effective refractive index $n$ on the wave profiles. The wave intensity and the field penetration depth in the hyperbolic graded-index crystal reduce with the increasing value of $n$.

Figure 1b demonstrates the influence of the interface refractive index $n_0$ on the wave profiles. The wave intensity increases with the increasing value of $n_0$. The field penetration depth in the hyperbolic graded-index crystal increases slightly in this case. The oscillation period in the photorefractive crystal $\Lambda$ increases. Increasing the characteristic distance $h$ leads to the same effects (Fig. 1c).

A temperature variation changes the wave profile only in the photorefractive crystal, while in the hyperbolic graded-index crystal it remains unchanged (Fig. 1d). The intensity of the peaks increases, the period of oscillations in the photorefractive crystal does not change with increasing temperature.

It is important to note that obtained equations (3.8), and (3.9) describe the waves, the spatial transverse profile of which can attenuate with oscillations in the hyperbolic graded-index crystal and not only in the photorefractive crystal. The wave oscillating profiles of the first type given by equation (3.8) in both crystals are shown in Figure 1e. Oscillations occur when the characteristic distance $h$ (or interface refractive index $n_0$) increases. t is obvious that the formation of oscillations in a hyperbolic graded-index crystal is associated with self-reflection of waves from layers with a decreasing refractive index [17]. With increasing values of the hyperbolic profile parameters, the period and amplitude of oscillations, as well as the depth of field penetration in the hyperbolic graded-index crystal, increase.

Figures 2–4 demonstrate the system parameter influence such as the effective refractive index $n$, characteristic distance of the hyperbolic profile $h$, temperature $T$ respectively on the total power flow $P$ carried by the interface

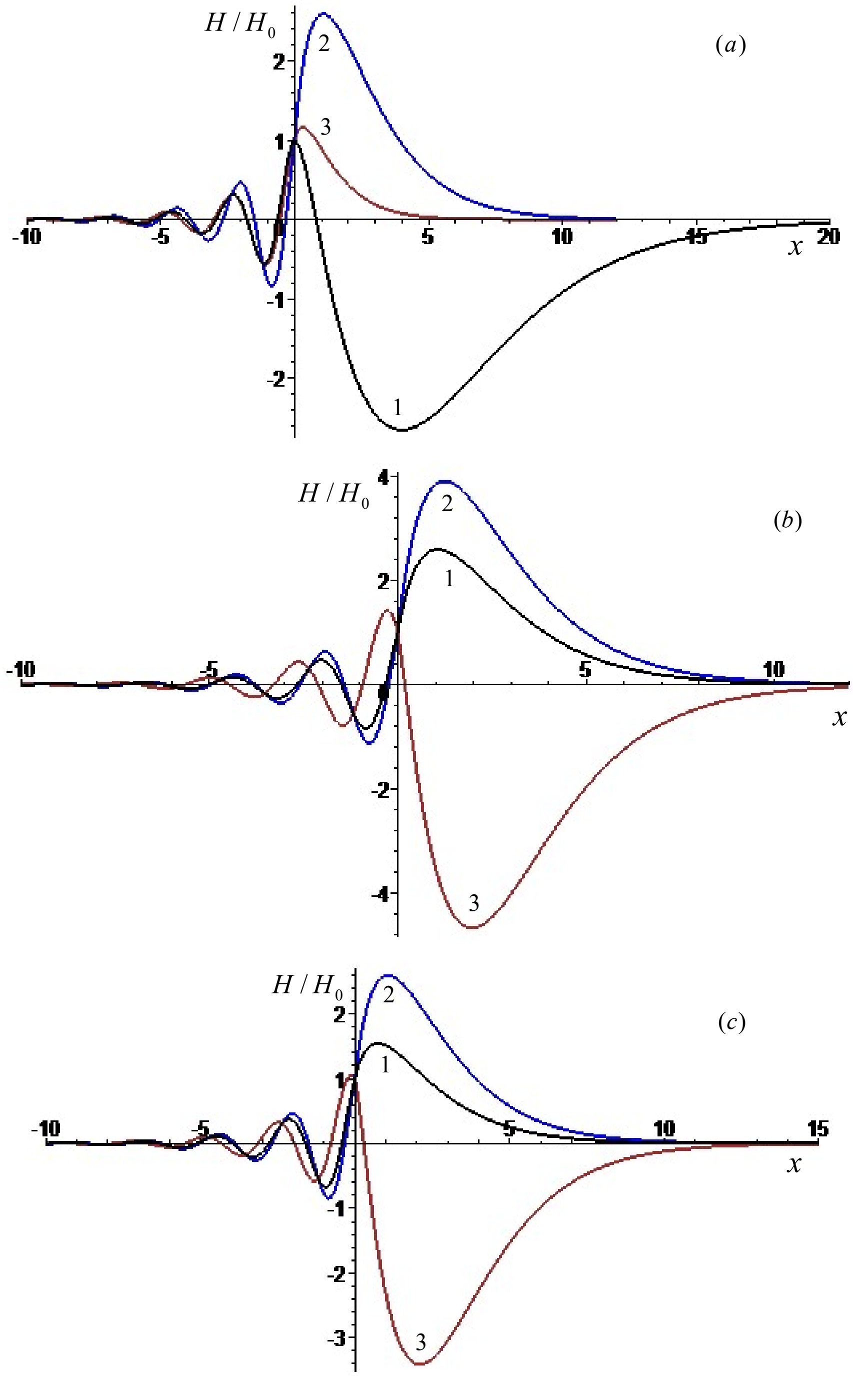


FIGURE 1. Transverse profiles on the interface waves of the first type $H(x)/H_0$ given by equation (3.8) (in dimensionless conventional units) with $k_0 = 0.7$, $n_{p0} = 4$, (a) $T = 0.5T_p/k_0$, $h = 0.1$, $n_0 = 5$, $n = 0.6$, (1), $n=1$ (2), $n=1.5$ (3); (b) $T=0.5T_p/k_0$, $n=1$, $n_0=5$, $h=0.1$ (1), $h=0.11$ (2), $h=0.15$ (3); (c) $T=0.5T_p/k_0$, $n=1$, $h=0.1$, $n_0=4.5$ (1), $n_0=5$ (2), $n_0=6.2$ (3); (d) $n_0=5$, $n=1$, $h=0.1$, $T=0.3T_p/k_0$ (1), $T=0.5T_p/k_0$ (2), $T=0.7T_p/k_0$ (3); (e) $T=0.5T_p/k_0$, $n=1$, $n_0=5$, $h=0.1$ (1), $h=0.3$ (2), $h=0.45$ (3).

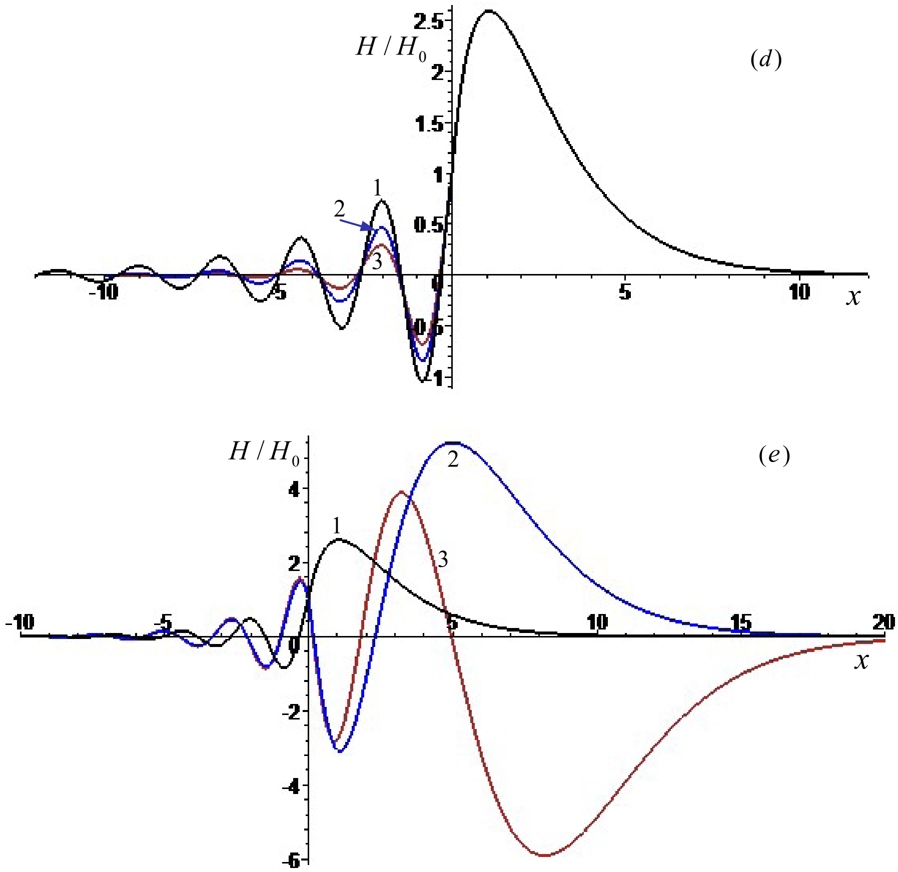


FIGURE 1. Continued.

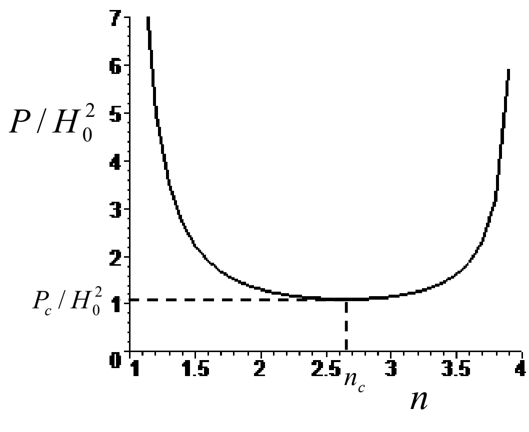


FIGURE 2. The total power flow carried by the interface wave of the first type with the components given by equations (3.13), and (3.14) *versus* the effective refractive index $n$ with $n < n_b$ and $k_0 = 0.7$, $n_p0 = 4$, $T = 0.5T_p/k_0$, $h = 0.1$, $n_0 = 5$ (in dimensionless conventional units).

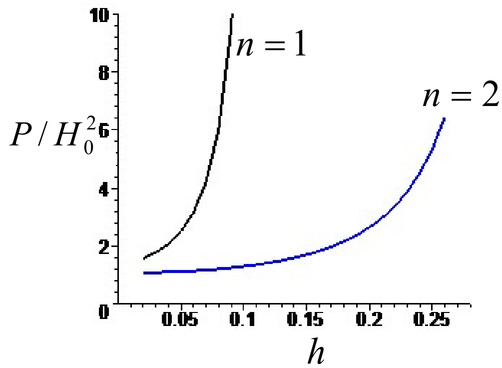


FIGURE 3. The total power flow carried by the interface wave of the first type with the components given by equations (3.13), and (3.14) *versus* the characteristic distance $h$ with $n < n_b$ and $k_0 = 0.7$, $n_{p0} = 4$, $T = 0.5T_p/k_0$, $n_0 = 5$ (in dimensionless conventional units).

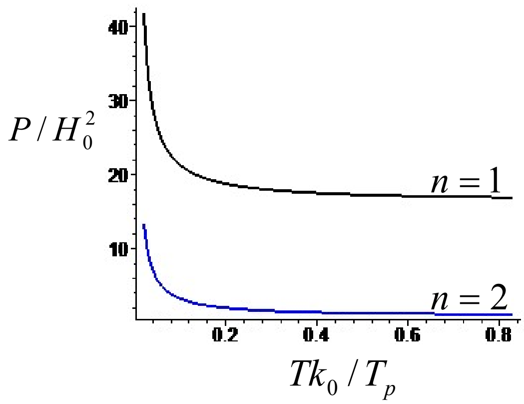


FIGURE 4. The total power flow carried by the interface wave of the first type with the components given by equations (3.13), and (3.14) *versus* the temperature $T$ with $n < n_b$ and $k_0 = 0.7$, $n_{p0} = 4$, $h = 0.1$, $n_0 = 5$ (in dimensionless conventional units).

wave of the first type with $n < n_b$. We observe the minimum value of $P_c$ at the critical effective refractive index $n_c$ (Fig. 2). This dependence is typical, since the excitation of the interface wave requires a current power exceeding the critical value of $P_c$ [64–66].

The total power flow increases monotonically with the increasing value of the characteristic distance $h$ (or interface refractive index $n_0$) (Fig. 3), and it decreases monotonically with the increasing value of the temperature (Fig. 4).

Figures 5–7 demonstrate the system parameter influence on the confinement factors $\Gamma_j$ $(j = hy, ph)$ of the interface wave of the first type with $n < n_b$. The confinement factors $\Gamma_{hy}$ in the hyperbolic graded-index crystal decreases and confinement factors $\Gamma_{ph}$ in the photorefractive crystal increases with the increasing value of effective refractive index $n$ (Fig. 5). We find the value of the effective refractive index $n_e$ (Fig. 5), at which both confinement factors coincide with each other: $\Gamma_{hy}(n_e) = \Gamma_{ph}(n_e)$. We observe that at small values of $n$ not exciding the value of $n_e$, the energy density is concentrated in the hyperbolic graded-index crystal while $\Gamma_{hy}(n) > \Gamma_{ph}(n)$. Then with the further increasing effective refractive index energy density is redistributed into the photorefractive crystal while $n > n_e$ and $\Gamma_{hy}(n) < \Gamma_{ph}(n)$.

The dependencies of the factors $\Gamma_j(j = hy, ph)$ of the interface wave of the first type with $n < n_b$ on the characteristic distance of the hyperbolic profile $h$, is presented in Figure 6. Basically, the energy density is

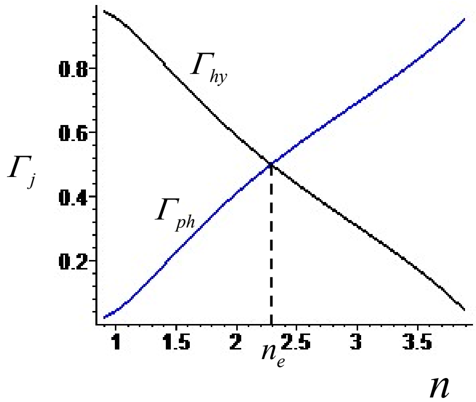


FIGURE 5. The confinement factors $\Gamma_j$ $(j = hy, ph)$ of the interface wave of the first type with the components given by equations (3.13), and (3.14) *versus* the effective refractive index $n$ with $n < n_b$ and $k_0 = 0.7$, $n_{p0} = 4$, $T = 0.5T_p/k_0$, $h = 0.1$, $n_0 = 5$ (in dimensionless conventional units).

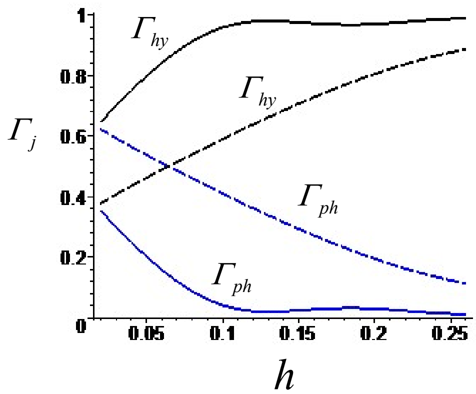


FIGURE 6. The confinement factors $\Gamma_j$ $(j = hy, ph)$ of the interface wave of the first type with the components given by equations (3.13), and (3.14) *versus* the characteristic distance $h$ with $n < n_b$ and $k_0 = 0.7$, $n_{p0} = 4$, $T = 0.5T_p/k_0$, $n_0 = 5$, $n = 1$ (solid lines) $n = 2$ (dashed lines) (in dimensionless conventional units).

concentrated in the hyperbolic graded-index crystal. However, at high values of the effective refractive index, regions of small values of $h$ appear, at which the energy density is concentrated in the photorefractive crystal. However, with a further increase in the values of $h$, a redistribution of the energy density from the photorefractive to the hyperbolic graded-index crystal is observed. The influence of the interface refractive index $n_0$ is completely analogous.

Similar conclusions can be made regarding the effect of temperature on the redistribution of the energy density flow between the crystals. As the temperature increases, the main part of the energy is concentrated in the hyperbolic graded-index crystal (Fig. 7).

Characteristic profiles of the interface waves of the second type given by equation (3.9) are presented in Figure 8. Note that the attenuation of the field profile of the second type of waves into the depth of a photorefractive crystal can be monotonous one or it can have one maximum or minimum. In particular, the one field maximum is located in the hyperbolic graded-index crystal at small values of the effective refractive index and its height reduces with increasing the value of $n$ (lines 1 and 2 in Fig. 8a). Then, the field maximum moves into

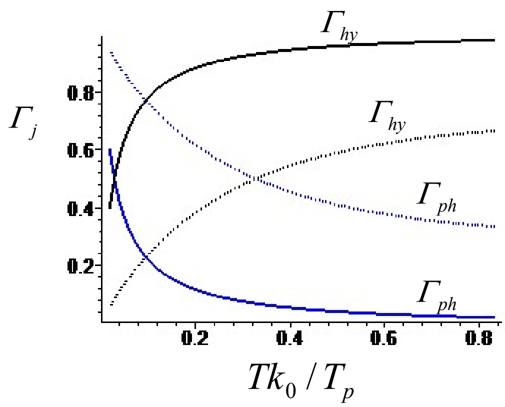


FIGURE 7. The confinement factors $\Gamma_j$ $(j = hy, ph)$ of the interface wave of the first type with the components given by equations (3.13), and (3.14) *versus* the temperature $T$ with $n < n_b$ and $k_0 = 0.7$, $n_{p0} = 4$, $h = 0.1$, $n_0 = 5$, $n = 1$ (solid lines) $n$=2 (dashed lines) (in dimensionless conventional units).

the photorefractive crystal with further increase of $n$ (line 3 in Fig. 8a). The depth of field penetration into the hyperbolic graded-index crystal is significantly reduced in this case.

A change from the maximum of the field profile to a minimum can be observed in a photorefractive crystal, which can be regulated by the parameters of the hyperbolic profile. Figure 8b demonstrates such a transition occurring with an increase in the characteristic distance $h$ (line 3 in Fig. 8b). We observe also an increase in the field intensity and penetration depth in the hyperbolic graded-index crystal with the increasing value of $h$ (lines 1 and 2 in Fig. 8b). Similar effects appear with increasing interface refractive index $n_0$ (lines 1 and 2 in Fig. 8c). However, one can also observe a change from the maximum of the field distribution profile to a minimum in a hyperbolic graded-index crystal with increasing $n_0$ (line 3 in Fig. 8c).

A temperature variation changes the profile of second type wave (just like the first type wave) only in the photorefractive crystal, while in the hyperbolic graded-index crystal it remains unchanged (Fig. 8d). The field penetration depth in the photorefractive crystal reduces with an increasing temperature.

Spatial profile oscillations may appear in waves of the second type just as for waves of the first type with increasing values of the parameters of the hyperbolic profile. Figure 8e demonstrates such a phenomenon occurring with an increase in the interface refractive index $n_0$.

The analysis of the power flows of waves of the second type showed that the influence of the system parameters on them is completely analogous to waves of the first type. It does not bring anything new and therefore does not require a detailed description.

## 5. Conclusion

We described theoretically the new two types of transverse interface waves propagating along the planar contact the photorefractive and hyperbolic graded-index crystals. The photorefractive nonlinearity is characterized by diffusion mechanism of optical response formation when the dark intensity is negligibly small compared to the intensity of the wave field. The waves of the two types differ from each other by the presence of oscillations of the decaying field profile in the photorefractive crystal and the range of existence (the permissible interval of values of the effective refractive index).

The interface waves are described by exact analytical solutions to the stationary wave equations with spatial dependent coefficients, which are given by the Whittaker function. We analyzed in details the influence on the wave profiles of the system parameters such as the effective refractive index, temperature, and the hyperbolic profile parameters: the interface refractive index, and the characteristic distance. We identified new features of

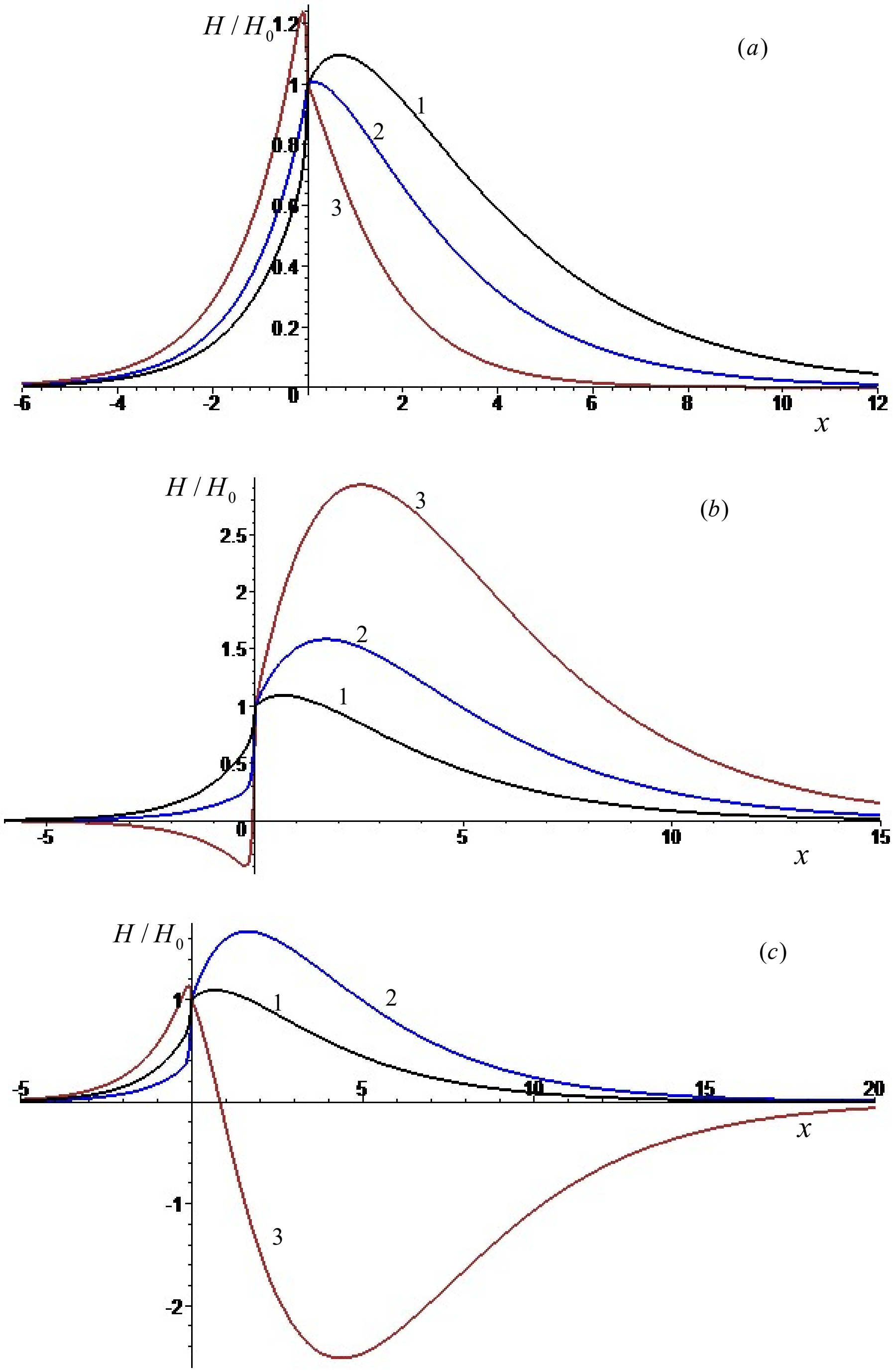


FIGURE 8. Transverse profiles on the interface waves of the second type $H(x)/H_0$ given by equation (3.9) (in dimensionless conventional units) with $k_0 = 1$, $n_{p0} = 4$, (a) $T = 10T_p/k_0$, $h = 0.5$, $n_0 = 1$, $n = 0.4$, (1), $n = 0.5$ (2), $n = 0.8$ (3); (b) $T = 10T_p/k_0$, $n = 0.4$, $n_0 = 1$, $h = 0.5$ (1), $h = 0.8$ (2), $h = 1.02$ (3); (c) $T = 10T_p/k_0$, $n = 0.4$, $h = 0.5$, $n_0 = 1.0$ (1), $n_0 = 1.2$ (2), $n_0 = 1.6$ (3); (d) $n_0 = 1$, $n = 0.4$, $h = 0.5$, $T = 5T_p/k_0$ (1), $T = 11T_p/k_0$ (2), $T = 20T_p/k_0$ (3); (e) $T = 10T_p/k_0$, $n = 0.4$, $h = 0.5$, $n_0 = 1.0$ (1), $n_0 = 1.8$ (2), $n_0 = 2.14$ (3).

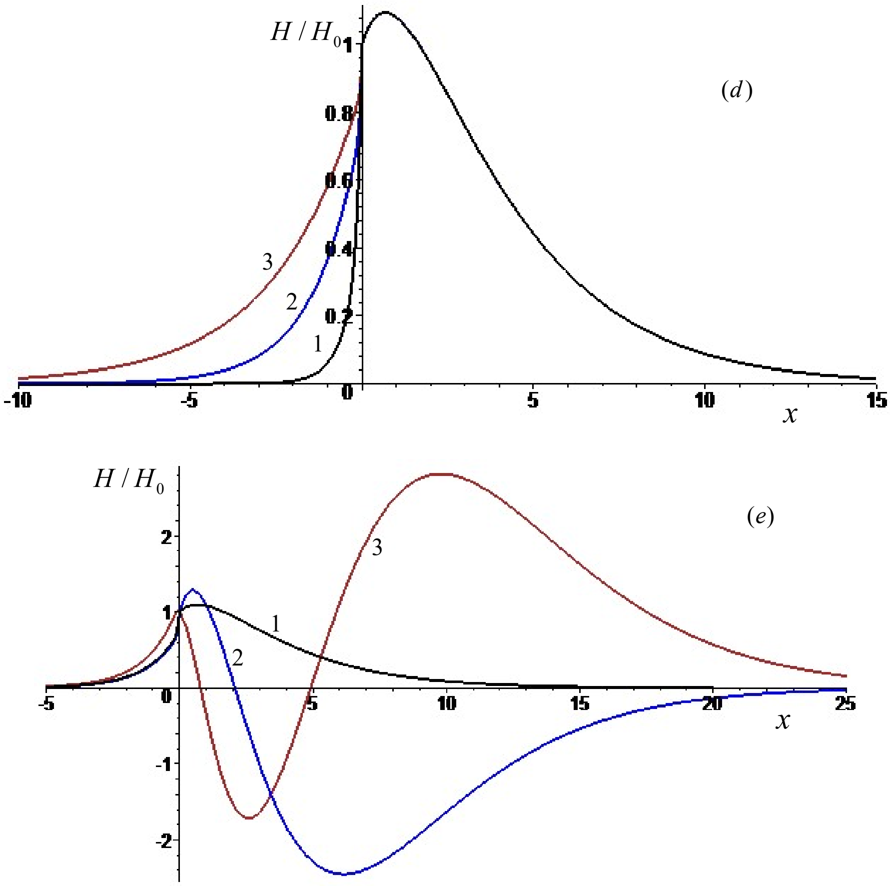


Figure 8. Continued.

the distribution of the maxima and minima of the field profile and the depth of its penetration into crystals depending on the values of these parameters.

We calculated and analyzed the power flows and confinement factors, using of which we identified the areas of the crystal along the waveguide, in which the magnitude of the power flow of the interface wave will be the greatest one.

The results of this paper complement previously studies of the features of the propagation of surface waves in photorefractive crystals and in graded-index media, taking into account the specifics of the decrease in the refractive index inversely proportional to the distance from the surface. The results of the paper also expand theoretical understanding of the mechanisms of formation of surface waves along the boundaries of nonlinear and inhomogeneous optical media and its possible applications [57].

## Conflits of interest

The author declares that he has no known competing financial interests or personal relationships that could have appeared to influence the work reported in this paper.

## Data availability statement

All data that support the findings of this study are included within the article.

## Author contribution statement

Author wrote this paper and contributed with analytical calculations supplemented by graph data.

## References


[1] B.A. Malomed and D. Mihalache, Nonlinear waves in optical and matter-wave media: a topical survey of recent theoretical and experimental results. *Rom. Jo. Phys.* **64** (2019) 106.

[2] D. Mihalache, Localized structures in optical and matter-wave media: a selection of recent studies. *Roman. Rep. Phys.* **73** (2021) 403.

[3] D. Mihalache, Localized structures in optical media and Bose–Einstein condensates: an overview of recent theoretical and experimental results. *Roman. Rep. Phys.* **76** (2024) 402.

[4] S.M. Shandarov and E.S. Shandarov, Photorefractive slit waves. *Tech. Phys. Lett.* **23** (1997) 586–588.

[5] T.H. Zhang, X.K. Ren, B.H. Wang, C.B. Lou, Z.J. Hu, W.W. Shao, Y.H. Xu, H.Z. Kang, J. Yang, D.P. Yang, L. Feng and J.J. Xu, Surface waves with photorefractive nonlinearity. *Phys. Rev. A* **76** (2007) 013827.

[6] Z. Luo, F. Liu, Y. Xu, H. Liu, T. Zhang, J. Xu and J. Tian, Dark surface waves in self-focusing media with diffusion and photovoltaic nonlinearities. *Opt. Express*, **21** (2013) 15075–15080.

[7] P.F. Qi, Z.J. Hu, R. Han, T.H. Zhang, J.G. Tian and J.J. Xu, Apodized waveguide arrays induced by photorefractive nonlinear surface waves. *Opt. Express* **23** (2015) 31144–31149.

[8] L. Chun-Yang, J. Ying, S. De, M. Yi-Ning, Y. Ji-Kai and C. Wei-Jun, Guided modes in thin layer waveguide induced by photorefractive surface waves. *Chinese J. Luminescence* **39** (2018) 1572–1578.

[9] S.E. Savotchenko, Propagation of surface waves along a dielectric layer in a photorefractive crystal with a diffusion mechanism for the nonlinearity formation. *Quant. Electron.* **49** (2019) 850–856.

[10] S.E. Savotchenko, Nonlinear surface TM waves in a Kerr defocusing nonlinear slab sandwiched between photorefractive crystals. *Solid State Commun.* **296** (2019) 32–36.

[11] S.E. Savotchenko, Nonlinear surface waves at the interface between optical media with different nonlinearity induction mechanisms. *JETP* **129** (2019) 159–167.

[12] S.E. Savotchenko, Effect of the dark illumination intensity on the characteristics of surface waves propagating along the interface between photorefractive and nonlinear Kerr crystals. *Russ. Phys. J.* **63** (2020) 160–170.

[13] S.E. Savotchenko, Surface waves at the boundary of a photorefractive crystal and a medium with positive Kerr nonlinearity. *Phys. Solid State* **62** (2020) 1011–1016.

[14] S.E. Savotchenko, Surface waves at the boundary of a medium with a refractive index switching and a crystal with the diffusion-type photorefractive nonlinearity. *Phys. Solid State* **62** (2020) 1415–1420.

[15] B.A. Usievich, D.Kh. Nurligareev, V.A. Sychugov, L.I. Ivleva, P.A. Lykov and N.V. Bogodaev, Nonlinear surface waves on the boundary of a photorefractive crystal. *Quant. Electron.* **40** (2010) 437–440.

[16] S.A. Chetkin and I.M. Akhmedzhanov, Optical surface wave in a crystal with diffusion photorefractive nonlinearity. *Quant. Electron.* **41** (2011) 980–985.

[17] B.A. Usievich, D.Kh. Nurligareev, V.A. Sychugov, L.I. Ivleva, P.A. Lykov and N.V. Bogodaev, Surface photorefractive wave on the boundary of a photorefractive metal-coated crystal. *Quant. Electron.* **41** (2011) 262–266.

[18] D.Kh. Nurligareev, B.A. Usievich, V.A. Sychugov and L.I. Ivleva, Characteristics of surface photorefractive waves in a nonlinear SBN-75 crystal coated with a metal film. *Quant. Electron.* **43** (2013) 14–20.

[19] A.B. Shvartsburg and A. Maradudin, Waves in Gradient Metamaterials. World Scientific, Singapore (2013) 339.

[20] S.J. Al-Bader and H.A. Jamid, Graded-index optical waveguides with nonlinear cladding. *J. Opt. Soc. Am. A* **5** (1988) 374–379.

[21] M.J. Adams, An Introduction to Optical Waveguides. Wiley, Chichester (1981).

[22] C.-L. Chen, Foundations for Guided-wave Optics. John Wiley & Sons, Inc. (2005) 462.

[23] P. D'Ancona, Kato smoothing and strichartz estimates for wave equations with magnetic potentials. *Commun. Math. Phys.* **335** (2015) 1–16

[24] F. Cacciafesta, P. D'Ancona and R. Lucà, Renato Helmholtz and dispersive equations with variable coefficients on exterior domains. *SIAM J. Math. Anal.* **48** (2016) 1798–1832.

[25] A.D. Polyanin and A.I. Zhurov, Separation of Variables and Exact Solutions to Nonlinear PDEs. CRC Press, Taylor and Francis Group, LLC, Boca Raton, London (2022) 382.

[26] Z. Cao, Y. Jiang, Q. Shen, X. Dou and Y. Chen, Exact analytical method for planar optical waveguides with arbitrary index profile. *J. Opt. Soc. Am. A* **16** (1999) 2209–2212.

[27] N.A. Kudryashov, Optical solitons of mathematical model with arbitrary refractive index. *Optik* **224** (2020) 165391.

[28] N.A. Kudryashov, Optical solitons of the Chen–Lee–Liu equation with arbitrary refractive index. *Optik* **247** (2021) 167935.

[29] G. Akram, M. Sadaf and I. Zainab, The dynamical study of Biswas-–Arshed equation via modified auxiliary equation method. *Optik* **255** (2022) 168614.

[30] N.A. Kudryashov and A. Biswas, Optical solitons of nonlinear Schrödinger's equation with arbitrary dual-power law parameters. *Optik* **252** (2022) 168497.

[31] N.A. Kudryashov, Stationary solitons of the model with nonlinear chromatic dispersion and arbitrary refractive index. *Optik* **259** (2022) 168888.

[32] S.A. Odintsov, E.H. Lock, E.N. Beginin and A.V. Sadovnikov, Nonreciprocal propagation of spin waves in a bilayer magnonic waveguide based on yttrium-iron garnet films. *Russ. Technol. J.* **10** (2022) 55–64.

[33] Y. Yıldırım, A. Biswas, A.H. Kara, M. Ekici, E.M.E. Zayed, A.K. Alzahrani and M.R. Belic, Optical solitons and conservation law with Kudryashov's form of arbitrary refractive index. *J. Opt. (India)* **50** (2021) 542–547.

[34] E.M.E. Zayed, A.G. Al-Nowehy, M.E.M. Alngar, A. Biswas, M. Asma, M. Ekici, A.K. Alzahrani and M.R. Belic, Highly dispersive optical solitons in birefringent fibers with four nonlinear forms using Kudryashov's approach. *J. Opt. (India)* **50** (2021) 120–131.

[35] J. Vega-Guzman, A. Biswas, M. Asma, A.R. Seadawy, M. Ekici, A.K. Alzahrani and M.R. Belic, Optical soliton perturbation with parabolic–nonlocal combo nonlinearity: undetermined coefficients and semi-inverse variational principle. *J. Opt. (India)* **51** (2022) 22–28.

[36] A. Jawad and M. Abu-AlShaeer, Highly dispersive optical solitons with cubic law and cubic-quintic-septic law nonlinearities by two methods. *Rafidain J. Eng. Sci.* **1** (2023) 1–8.

[37] M. Jawad A. Jafar, Y. Yildirim, A. Biswas, I.K. Ibraheem and A.S. Alshomrani, Highly dispersive optical solitons with differential group delay for kerr law of self-phase modulation by Sardar sub-equation approach. *Contemp. Math.* **5** (2024) 3839–383957.

[38] A.J.M. Jawad, A. Biswas, Y. Yildirim and A.S. Alshomrani, Highly dispersive optical solitons with quadratic-cubic nonlinear form of self-phase modulation by Sardar sub-equation approach. *Contemp. Math.* **5** (2024) 1300–1322.

[39] N. Jihad and M. Abd Almuhsan, Evaluation of impairment mitigations for optical fiber communications using dispersion compensation techniques. *Rafidain J. Eng. Sci.* **1** (2023) 81–92.

[40] A.J.M. Jawad, A. Biswas, Y. Yıldırım and A.S. Alshomrani, A fresh perspective on the concatenation model in optical fibers with Kerr law of self-phase modulation. *Eng. Sci. Technol.* **5** (2024) 195–208.

[41] A.J.M. Jawad, A. Biswas, Y. Yildirim and A.S. Alshomrani, Dark-singular straddled optical solitons for the dispersive concatenation model with power-law of self-phase modulation by Tanh-Coth approach. *Contemp. Math.* **5** (2024) 3198–3214.

[42] A. Jawad and A. Biswas, Solutions of resonant nonlinear Schrödinger's equation with exotic non-Kerr law nonlinearities. *Rafidain J. Eng. Sci.* **2** (2023) 43–50.

[43] T. Aytug, A. Lupini, G. Jellison, P.C. Joshi, I. Ivanov, T. Liu, P. Wang, R. Menon, R. Trejo, E. Lara-Curzio, S. Hunter, J. Simpson, P. Paranthaman and D. Christen, Monolithic graded-refractive-index glass-based antireflective coatings: broadband/omnidirectional light harvesting and self cleaning characteristics. *J. Mater. Chem. C* **3** (2015) 5440.

[44] J. Zheng, W. Zhao, B. Zhao, C. Hou, Z. Li, G. Li, Q. Gao, P. Ju, W. Gao, S. She, P. Wu and W. Li, 4.62 kW excellent beam quality laser output with a low-loss Yb/Ce co-doped fiber fabricated by chelate gas phase deposition technique. *Opt. Mater. Express* **7** (2017) 1259–1266.

[45] F. Gaufillet and E. Akmansoy, Design and experimental evidence of a flat graded-index photonic crystal lens. *J. Appl. Phys.* **114** (2013) 083105.

[46] H. Rauh, G.I. Yampolskaya and S.V. Yampolskii, Optical transmittance of photonic structures with linearly graded dielectric constituents. *New J. Phys.* **12** (2010) 073033.

[47] K. Ratra, M. Singh and A.K. Goyal, Design and analysis of omni-directional solar spectrum reflector using one-dimensional photonic crystal. *J. Nanophoton.* **14** (2020) 026005.

[48] Y.B. Kim, J.W. Cho, Y.J. Lee, B. Dukkyu and S.-K. Kim, High-index-contrast photonic structures: a versatile platform for photon manipulation. *Light Sci. Appl.* **11** (2022) 316.

[49] B.K. Singh, A. Bijalwan, P.C. Pandey and V. Rastogi, Photonic bandgaps engineering in double graded hyperbolic, exponential and linear index materials embedded one-dimensional photonic crystals. *Eng. Res. Express* **1** (2019) 025004.

[50] B.K. Singh, A. Bijalwan, P.C. Pandey and V. Rastogi, Multi-channel photonic bandgap consequences in one-dimensional linear, exponential, and hyperbolic graded-index photonic crystals. *J. Opt. Soc. Am. B* **37** (2020) 523.

[51] D. Dash and J. Saini, Hyperbolic graded index biophotonic cholesterol sensor with improved sensitivity. *Progr. Electromagnet. Res. M* **116** (2023) 165–176.

[52] P. Yeh, Optical Wave in Layered Media. Wiley, New Jersey (1988).

[53] S.E. Savotchenko, The surface waves propagating along the contact between the layer with the constant gradient of refractive index and photorefractive crystal. *J. Opt.* **24** (2022) 045501.

[54] S.E. Savotchenko, Waveguide properties of interface separating a photorefractive crystal with diffusion nonlinearity and an exponential graded-index medium. *Phys. Lett. A* **455** (2022) 128516.

[55] S.E. Savotchenko, Surface waves propagating along the interface between parabolic graded-index medium and photorefractive crystal with diffusion nonlinearity. *Physica B: Condensed Matter* **648** (2023) 414434.

[56] S.E. Savotchenko, Temperature controlled waveguide properties of the linearly graded-index film in semiconductor crystal with the photorefractive nonlinearity. *Appl. Phys. B: Lasers Opt.* **129** (2023) 7.

[57] S.E. Savotchenko, The effect of dielectric slab between photorefractive crystal and graded-index medium on the surface wave properties. *Physica E* **147** (2023) 115622.

[58] S.E. Savotchenko, Nonlinear waves in a composite optical structure containing a dielectric layer between a photorefractive crystal and a medium with an exponential index profile. *Waves in Random and Complex Media* (2023).

[59] S.E. Savotchenko, Nonlinear surface waves propagating along an interface between the Kerr nonlinear and hyperbolic graded-index crystals. *J. Opt. (India)* **53** (2024).

[60] S.E. Savotchenko, Features of the surface wave propagation along the interface between the hyperbolic graded-index layer and nonlinear medium with a step change in the dielectric constant. *Phys. Lett. A* **524** (2024) 129822.

[61] S.E. Savotchenko, Effect of the temperature on the redistribution of an energy flux carried by surface waves along the interface between crystals with different mechanisms of formation of a nonlinear response. *JETP Lett.* **109** (2019) 744–748.

[62] W. Van Assche, Ordinary Special Functions. *Encyclopedia of Mathematical Physics*, edited by J.-P. Françoise, G. L. Naber and T.S. Tsun. Academic Press, New York (2006) 637–645.

[63] V.K. Chaubey, K.K. Dey and P. Khastgir, Field intensity and power confinement of four-layer slab waveguides with various refractive index profiles in the guiding region. *J. Opt. Commun.* **15** (1994) 95–100.

[64] L.V. Fedorov and K.D. Ljahomskaja, Nonlinear surface waves with allowance for the saturation effect. *Tech. Phys. Lett.* **23** (1997) 915–916.

[65] O.V. Korovai and P.I. Khadzhi, Nonlinear asymmetric waves induced in a symmetrical three-layer structure by the generation of excitons and biexcitons in semiconductors. *Phys. Solid State* **50** (2008) 1116–1120.

[66] O.V. Korovai, Nonlinear s-polarized quasi-surface waves in the symmetric structure with a metamaterial core. *Phys. Solid State* **57** (2015) 1456–1462.